



Adsorption of Cd(II) From Aqueous Solutions by Modified Biochars: Comparison of Modification Methods

Yue Qiu · Qian Zhang · Meng Li · Zixi Fan · Wenjiao Sang · Chenfeiyang Xie · Dongyuan Niu

Received: 21 November 2018 / Accepted: 7 March 2019 / Published online: 20 March 2019
© Springer Nature Switzerland AG 2019

Abstract In this study, adsorption experiments on Cd(II) ions in aqueous solution by biochars pyrolyzed from millet bran (MBBC) at 400–800 °C were carried out and MBBC had superior adsorption performance at pyrolysis temperature of 600–800 °C. Then, biochars were modified by potassium permanganate (MBBC-PP), potassium ferrate (MBBC-PF), and citric acid (MBBC-CA). The results showed that the adsorption capacities of these adsorbents were in the order: MBBC-PP > MBBC-PF > MBBC-CA > MBBC. FT-IR, XRD, and Raman were used to determine the characteristics of biochars and explore the main adsorption mechanism causing by modification. These characterizations confirmed that manganese oxide and iron oxide particles were loaded on the surface of MBBC-PP and MBBC-PF, respectively. For MBBC-PP and MBBC-PF, the adsorption sites generated by the loaded metal oxides play more important role than other factors in Cd(II) adsorption. For MBBC-CA, surface functional groups were the main contributor during Cd(II) adsorption. Batch

adsorption experiments demonstrate a Langmuir model fit for Cd(II). The sorption kinetics of Cd(II) on adsorbents follows pseudo-second-order kinetics. Modified biochars, especially the one modified by KMnO₄, could act as effective alternatives to enhance heavy metals removal from aqueous solutions.

Keywords Biochar · Modification · Adsorption · Cd(II) · Mechanism

1 Introduction

Rapid advance of industrialization and urbanization causes serious environmental issues, which include a large amount of industrial effluents containing heavy metals (Barakat 2011). Cadmium (Cd) has been considered as one of the most toxic and non-biodegradable heavy metals, which can be emitted into the aquatic ecosystem and accumulated in the food chain through industrial effluents, posing serious threats to aquatic organism and human health. Cd could cause various types of disorders and even have a carcinogenesis (Bagchi et al. 2017; Yang et al. 2018). Hence, ecofriendly and sustainable suggestions are needed urgently, for eliminating Cd contamination from the aqueous environment.

Numerous Cd(II)-contaminated wastewater treatment techniques include chemical precipitation, membrane separation, ultrafiltration, electrolytic recovery, and ion exchange (Chen et al. 2018; Ni et al. 2018). However, these techniques have their inherent limitations, such as high cost, sludge disposal, and secondary pollution (Fu

Electronic supplementary material The online version of this article (<https://doi.org/10.1007/s11270-019-4135-8>) contains supplementary material, which is available to authorized users.

Y. Qiu · Q. Zhang (✉) · M. Li · Z. Fan · W. Sang · C. Xie
School of Civil Engineering and Architecture, Wuhan University of Technology, Wuhan 430070, People's Republic of China
e-mail: qianzhang@whut.edu.cn

D. Niu
State Key Laboratory of Urban Water Resource and Environment, Harbin Institute of Technology, Harbin 150001, People's Republic of China

and Wang 2011; Won et al. 2014). Adsorption is regarded as a good alternative for heavy metal removal (Peng et al. 2017). Adsorption, especially, still works at medium or low ion concentrations (Inyang et al. 2012; Xin et al. 2015). However, the practical application of the well-known adsorbents like ion exchange resins and activated carbon are limited by their high expenditure and low efficiency (Wan et al. 2018). In recent years, biochars have garnered great attention as an ideal adsorbent for contaminant removal owing to its low cost and easy design (Demirbas 2008; Zhou et al. 2014).

Biochar produced by pyrolysis of biomass in an oxygen-limited environment is a kind of carbonaceous material with highly aromatization and recalcitrance (Fan et al. 2018; Sizmur et al. 2015). Biomass feedstock for biochar preparation has been extensively studied, including forestry wastes, agricultural waste, and industrial organic wastes, which can be utilized effectively and converted into valuable green by-products (Li et al. 2017a; Shan et al. 2015; Vafakhah et al. 2014). However, the adsorption ability of pristine biochars to remove contaminants is restricted due to the physicochemical properties of biochar (Li et al. 2017a).

Several studies indicated that chemically modified methodologies on feedstock or biochar increase the breadth of contaminants, including acids, bases, and metal oxides (Rajapaksha et al. 2016). So far, a number of methods for modifying biochar have been designed to enhance its adsorption capacity of Cd(II). Biochar modified by metal salts has been testified as a promising method (Wang et al. 2012). Xiang et al. (2018) successfully prepared rice husk biochar and magnesium oxide (MgO) composite using a MgO impregnation method and the adsorption capacity of Cd(II) was 18.1 mg/g. In previous studies, biochar modified by KMnO_4 impregnation to load manganese oxides have been found and demonstrated to be an effective modification method (Wang et al. 2015). Potassium ferrate, also as a strong oxidant, has not yet been extensively studied for Cd(II) removal. Potassium ferrate is a dark orchid powdered crystals with metallic luster and strong oxidizing, which has potential uses as a novel modifying agent. Additionally, acid modification is frequently applied to remove various pollutants and enhance adsorption capacity as well. Peng et al. (2017) carried out a simple modification of biochars by phosphoric acid (H_3PO_4) and found that the surface area was larger and the contents of oxygen-containing functional groups of modified biochars were more than pristine biochars.

Compared to strong acid frequently applied, citric acid is a kind of environment friendly organic acid, which could avoid secondary pollution of the environment during preparation (Sun et al. 2015). Several studies had already reported that citric acid could be applied to modify the surface of various biochars by introducing additional functional groups onto their surfaces, which may enhance their adsorption capacity (Xu et al. 2016). Thus, this study used potassium permanganate, potassium ferrate, and citric acid as the biochar modification agent to remove Cd(II) from aqueous solution and further determine their sorption mechanism.

Therefore, this study was aim to comprehensively evaluate several biochar modification methods for Cd(II) removal. Specifically, the objectives of this work were to (1) select three modification methods including KMnO_4 impregnation, K_2FeO_4 impregnation, and $\text{C}_6\text{H}_8\text{O}_7$ impregnation; (2) characterize the modified biochars and test their sorption capacities of Cd(II); and (3) comprehensively evaluate the mechanism governing the adsorption of Cd(II) on modified biochars.

2 Materials and Methods

2.1 Materials

Millet bran chosen as biochar feedstock were collected from Baotou City, Inner Mongolia, China. In order to ensure uniform heating of biomass for biochar preparation, the millet bran was washed and dried to constant weight and sieved after grinding, controlling the particle size in 0.8~0.15 mm. Potassium permanganate (158.03 g/mol, KMnO_4 ; 99.5%), potassium ferrate (198.04 g/mol, K_2FeO_4), citric acid monohydrate (210.14 g/mol, $\text{C}_6\text{H}_8\text{O}_7 \cdot \text{H}_2\text{O}$; 99.8%), and cadmium nitrate tetrahydrate (308.48 g/mol, $\text{Cd}(\text{NO}_3)_2 \cdot 4\text{H}_2\text{O}$; 99.0%) were purchased from Sinopharm Chemical Reagent Co., Ltd. (Shanghai, China). All chemicals and reagents were of analytical grade.

2.2 Modified Biochar Preparation

The prepared biomass was, respectively, pyrolyzed in a muffle furnace (SX2-5-12, Hubei JianLi Instrument Co., Ltd., China) at 400~800 °C for 2 h in an oxygen-limited environment. Then, the pristine biochars were collected and milled into particles with diameters

between 0.015 and 0.074 mm for the following adsorption experiments.

The millet bran feedstock was modified by KMnO_4 impregnation, K_2FeO_4 impregnation, and $\text{C}_6\text{H}_8\text{O}_7$ impregnation. Specific steps are as follows: 20 g millet bran was separately immersed using 250 mL of KMnO_4 (0.1 mol/L)/ K_2FeO_4 (0.1 mol/L)/ $\text{C}_6\text{H}_8\text{O}_7 \cdot \text{H}_2\text{O}$ (1 mol/L) solutions and stirred vigorously, followed by ultrasonication for 2 h to ensure uniform contact. After being oven dried, the biomass was milled, and sieved to particles with diameter between 0.15 and 0.80 mm and then pyrolyzed in a muffle furnace at 600 °C for 2 h under N_2 atmosphere. In order to exclude effects from ash component produced during heating process, the obtained biochar was washed three times with deionized water and dried at 80 °C overnight. The modified biochars were referred to as MBBC-PP, MBBC-PF, and MBBC-CA, where suffix letter PP, PF, and CA represent KMnO_4 , K_2FeO_4 , and $\text{C}_6\text{H}_8\text{O}_7$, respectively.

2.3 Batch Adsorption Experiments

A dosage of 100 mg biochars were added into 50 mL of solution containing 1 mmol/L Cd(II) concentration at initial pH 4.0. The biochar samples were shaken for 6 h in a constant temperature shaker at 160 rpm under 25 ± 1 °C conditions. After reaching the adsorption equilibrium, the reaction mixture was centrifuged for 15 min at the speed of 1500 rpm and filtrated through 0.20- μm microporous filter membrane. The residual concentration of Cd(II) ions was measured in the filtrate and determined by atomic absorption spectrophotometer (AAS; ZEE nit700P, Analytik-Jena, Germany). For the modified biochars, the effect of initial pH (2.0~7.0) on Cd(II) adsorption was investigated using the same procedure as described above.

An adsorption isotherm experiment was carried out by mixing 100 mg of adsorbent and 50 mL of aqueous solutions with different Cd(II) concentrations (0.16 to 6.00 mmol/L) for 24 h at 25 ± 1 °C. For adsorption kinetics, the mixture with 100 mg MBBC-PP and 50 mL of 1 mmol/L Cd(II) aqueous solutions was shaken at 25 ± 1 °C. Sampling time was set to 10, 20, 30 min, 1, 2, 3, 4, 6, 8, 12, and 24 h, respectively. The pH of Cd(II) solution was adjusted to around 5.5. Samples were immediately filtered and measured.

2.4 Analytical Methods

Surface functional groups on the biochars were identified by a Fourier transform infrared spectrometer (FT-IR; Nicolet 6700, Thermo Electron Scientific Inc., USA). Spectra were obtained in a wavelength range of 500~4000 cm^{-1} at a resolution of 0.019 cm^{-1} . X-ray diffraction (XRD) measurement was carried out to determine the crystalline structure and surface chemical composition of the adsorbents in a D8 Advance Bruker spectrometer by using $\text{Cu K}\alpha$ radiation with a scanning speed of 2°/min in the 2θ range between 10° and 80°. Raman spectra were recorded using a Renishaw Raman spectrometer (LabRam HR Evolution).

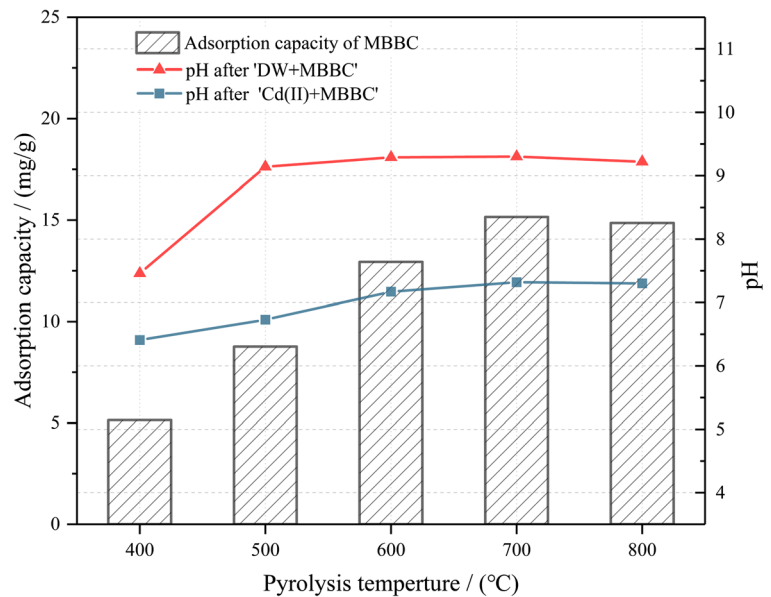
3 Results and Discussions

3.1 Cd(II) Adsorption of Pristine Biochars

Pyrolysis temperature is one of the most important factors affecting biochar structure and composition, and it can influence the adsorption characteristics of biochar by changing surface area, surface functionality, pore distribution, and mineral concentration of biochar (Ahmad et al. 2012; Chen et al. 2011; Kim et al. 2012). Adsorption capacities of pristine biochars (MBBC) toward Cd (II) were shown in Fig. 1. A higher pyrolysis temperature will promote better adsorption capacity of Cd(II) by biochar. The adsorption capacity reached the largest at biochar produced temperature of 700 °C. MBBC produced at 800 °C displayed a slightly decreased adsorption efficiency, which may be due to the less oxygen-containing functional groups or the blockage and collapse of the pore structure (Li et al. 2002; Paethanom and Yoshikawa 2012).

In order to study the effect of pyrolysis temperatures on pH and adsorption properties of MBBC, Cd(II) solution and deionized water (control experiment) were, respectively, mixed with appropriate amount of MBBC at an initial pH of 4.0. After shaking for 6 h, the pH values of the biochar suspension were detected. As shown in Fig. 1, the ash components on the biochar surface dissolved and released in the solution so that the pH tend to be neutral or alkaline from acidic, when MBBC was added into deionized water. It could be prone to find that biochar pH simultaneously increases with increasing pyrolysis temperature, which is mainly due to the increasing of contents of total base cations

Fig. 1 Effect of pyrolysis temperature on adsorption capacity of Cd(II) and pH values by pristine biochars. Experimental condition: MBBC = 100 mg, Cd(II) = 50 mL (1 mmol/L), DW = 50 mL, initial pH = 4.0, time = 6 h



and carbonates in biochar and the separation of alkali salts from organic matrix in the feedstock (Shinogi and Kanri 2003; Yuan et al. 2011). In addition, the reduction of O in biochar at high temperatures may lead to the disappearance of various acidic functional groups such as $-\text{COOH}$, resulting in a more alkaline surface of biochars (Al-Wabel et al. 2013; Li et al. 2002).

After Cd(II) adsorption, the pH of result solutions stabilized at 6.41~7.32, which were lower than that of control group. Kim et al. (2013) and Regmi et al. (2012) had reported that the removal of Cd(II) was significantly observed at pH 9.0 in the absence of biochars as a result of the formation of $\text{Cd}(\text{OH})_2$ precipitation. Hence, a hypothesis could be made that alkaline substances may be released from biochar and converted into precipitates by combining with Cd(II). Ion exchanges may occur during the process as well, that is, the surface functional groups of biochar complexed with Cd(II), replacing the hydrogen ions, resulting in a decrease in pH. Compared to the pristine biochar (MBBC) after a deash treatment in Fig. 2, the adsorption capacity was greatly improved, indicating that the Cd(II) removal was mainly dependent on the surface precipitation by ash component in the pristine biochar without deashing. It could be concluded from Fig. 1 that elevated temperature (600~800 °C) promotes the biochar surface to be alkaline and facilitates the removal of Cd(II). By deashing treatment, MBBC obtained at 600 °C exhibited relatively good

adsorption performance (data not shown). Therefore, 600 °C was chosen as the optimum pyrolysis temperature for subsequent studies.

3.2 Cd(II) Adsorption of Modified Biochars

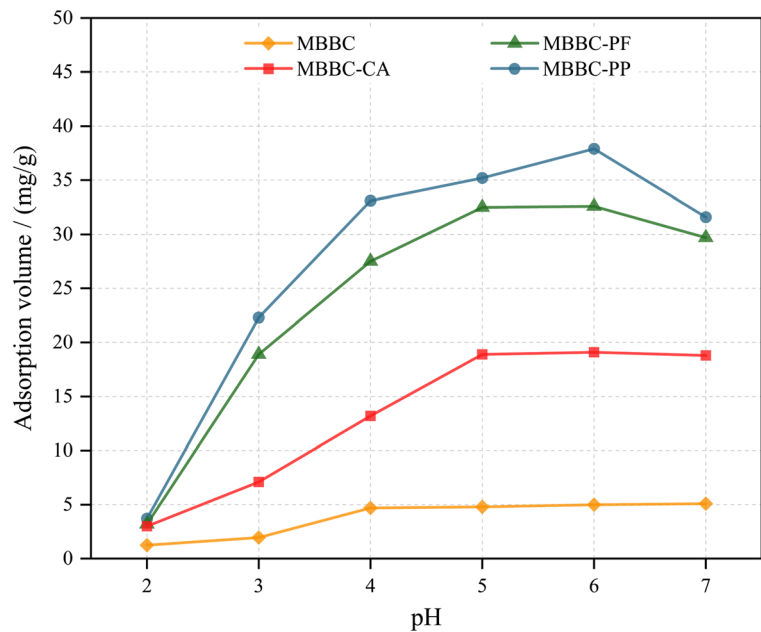
3.2.1 Adsorption Capacity of Cd(II) by Modified Biochars

Adsorption capacity of pristine biochar (MBBC) and modified biochars (MBBC-PP, MBBC-PF, MBBC-CA) were presented in Fig. S1. It could be clearly observed that all three modification methods greatly enhance adsorption capacity of Cd(II) from aqueous solutions compared with MBBC. Notably, the adsorption capacity of Cd(II) on MBBC-PP reached 22.51 mg/g approximately, which was five times than that of MBBC. MBBC-PF was second, and its adsorption capacity was increased to 18.65mg/g. The adsorption capacity of MBBC-CA was 12.47 mg/g, but still better than MBBC. The results indicated that modification methods indeed had a great influence on the adsorption properties of biochar, and KMnO_4 as oxidant modified biochar was more suitable to remove Cd (II) from aqueous solutions.

3.2.2 Effect of Initial pH

When biochar is applied for metal removal, solution initial pH strongly impacts biochar surface

Fig. 2 The effect of initial pH on Cd(II) adsorption by MBBC (washed), MBBC-PP, MBBC-PF, and MBBC-CA. Experimental condition: MBBC = 100 mg, Cd(II) = 50 mL (1 mmol/L), time = 6 h

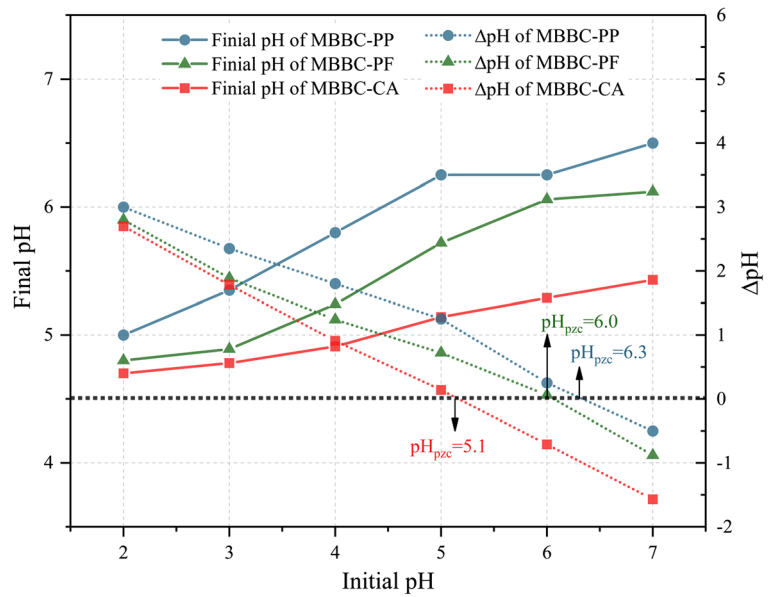


properties, surface charge, and metal speciation (Li et al. 2017c). Thus, the effects of initial solution pH on Cd(II) adsorption by MBBC, MBBC-PP, MBBC-PF, and MBBC-CA biochars were investigated at different pH ranging from 2.0 to 7.0. As shown in Fig. 2, it is clearly displayed that Cd(II) removal is pH-dependent. The removal efficiency of Cd(II) by MBBC-PP and MBBC-PF were significantly higher than those of MBBC and MBBC-CA, which could be attributed to the properties of different surface modifier. The adsorption capacities of MBBC-PP and MBBC-PF were observed to increase sharply when initial pH was increased from 2.0 to 6.0, and reached the maximum at pH 6.0. However, the adsorption capacity slightly decreased with a further increase of pH. In contrast, the adsorption capacity of MBBC and MBBC-CA increased slowly and stabilized when $\text{pH} > 4.0$.

To further illustrate the effects of pH, the zero point of charge (pH_{pzc}) of modified biochars was evaluated by reference to Jung et al. (2016), based on the ΔpH of pre- and post-adsorption. As shown in Fig. 3, the experimental pH_{pzc} for MBBC-PP, MBBC-PF, and MBBC-CA was 6.3, 6.0, and 5.1, respectively. When solution pH is lower than pH_{pzc} (6.3, 6.0, 5.1), biochar is positively charged and produces electrostatic repulsion that occurred between biochar and Cd(II) ions, preventing their

bonding. At the same time, excessive proton ions in solution strongly compete with Cd(II) for adsorption sites. In addition, MnO_x and FeO_x supported on biochar could dissolve into solution as free ions at low pH, thereby losing the possible complexation between metal oxides and Cd(II). This is why the adsorption capacity of all biochar is negligible at pH 2.0. With pH increasing from 3.0 to 5.0, the deprotonation of functional groups releases more binding sites, thus exhibiting an enhanced adsorption capacity. When solution pH is more than pH_{pzc} (6.3, 6.0, 5.1), biochar is negatively charged to bind with Cd(II) and the metal species on the biochar is presented in the form of oxides. The pH_{pzc} of MBBC-PF is smaller than that of MBBC-PP, which is consistent with the previous observation that the loading of iron oxide will increase the acidic groups on biochar surface (Li et al. 2017a). It can be seen from Fig. 2 that when the pH exceeds 6, the adsorption site of biochar has been fully occupied. Even if the biochar is negatively charged, the removal quantity of Cd(II) could not increase, which may be due to the formation of Cd(II) precipitates affecting the adsorption process. Therefore, the adsorption sites provided by MnO_x and FeO_x were more important than electrostatic interactions. MBBC-CA has the smallest pH_{pzc} (5.0), and when the solution pH is more than 5.0, the adsorption capacity did not significantly reduce,

Fig. 3 pH_{pzc} of MBBC-PP, MBBC-PF, and MBBC-CA



indicating that electrostatic interaction is one of the possible mechanisms.

3.2.3 Adsorption Isotherms and Kinetics

Langmuir and Freundlich equation models were used to fit the adsorption isotherms of Cd(II) adsorption by four biochars (MBBC, MBBV-PP, MBBC-PF, MBBC-CA) in this study. Langmuir and Freundlich equation models are described in the following Eqs. (1) and (2), respectively.

$$Q_e = \frac{Q_{max} b C_e}{1 + b C_e} \tag{1}$$

$$Q_e = k p^n \tag{2}$$

Q_e (mg/g) is the amount of metal adsorbed per unit weight of adsorbent, C_e (mg/L) is the equilibrium solution concentration phase of the adsorbate, Q_{max} is the maximum adsorption capacity (mg/g), b is the Langmuir constant related to the sorption energy (L/mg), n is the Freundlich constant related to surface heterogeneity, and K is the Freundlich constant related to sorption capacity ($mg^{1-n}L^n/g$).

Figure S2 shows curves of the adsorption capacities of the adsorbates as functions of Cd(II) solution equilibrium concentration. When the equilibrium solution concentration of Cd(II) was less than 50 mg/L, the

amount of Cd(II) adsorption was increased dramatically. On the other hand, when the equilibrium concentration of Cd(II) was greater than 100 mg/L, the amount of Cd(II) adsorption tended to plateau. Compared with the MBBC, the adsorption capacities of MBBC-PP, MBBC-PF, and MBBC-CA were 8.45, 7.32, and 3.65 times greater than that of MBBC, respectively. The adsorption capacities of these biochars were in the order: MBBC-PP > MBBC-PF > MBBC-CA > MBBC.

The Langmuir and Freundlich parameters and correlation coefficients (R^2) were known from Table S1. Obviously better fits were obtained using the Langmuir model than were obtained from the Freundlich model, suggesting that the mechanism of Cd(II) adsorption onto these biochars is more consistent with the Langmuir model. Therefore, the four adsorption behaviors mainly occurred in monolayers, including chemical and physical adsorption.

The pseudo-first-order and pseudo-second-order adsorption kinetic equation models were used to verify the sorption kinetics. Pseudo-first-order and pseudo-second-order adsorption kinetic equation models can be depicted in the following Eqs. (3) and (4), respectively.

$$\frac{dQ_t}{dt} = k_1(Q_e - Q_t) \tag{3}$$

$$\frac{dQ_t}{dt} = k_2(Q_e - Q_t)^2 \tag{4}$$

Q_e and Q_t (mg/g) are the amounts of Cd(II) adsorbed onto biochar at equilibrium and at extraction time, respectively; t (min) is the time; k_1 (min^{-1}) is the rate constant of pseudo-first-order model; and k_2 ($\text{g}/(\text{mg min})$) is the equilibrium rate constant of pseudo-second-order model.

Figure S3 illustrates the amounts of Cd(II) adsorbed by MBBC, MBBC-PP, MBBC-PF, and MBBC-CA, as functions of the contact time (0–24 h) and the parameters determined from two kinds of kinetic models for Cd(II) adsorption are listed in Table S2. Adsorption capacity of Cd(II) by four adsorbents increased with time and then stabilized as equilibrium was reached. The adsorption of Cd(II) was fast in the initial stages and then reached equilibrium after only 2 h, presumably because adsorption primarily occurs on the outer surfaces of these biochars. With increasing time, Cd(II) gradually diffuses into the carbon pores, further reacting with internal active sites of the carbon, where the adsorption process is relatively slow.

The kinetic adsorption data of Cd(II) was well fitted to the pseudo-second-order kinetic model, which can be seen from both the fitting curve and rate constants. The pseudo-second-order equation model provided high correlation coefficients with experimental results (R^2 equal to 0.982, 0.968, 0.989, and 0.993 for MBBC, MBBC-PP, MBBC-PF, and MBBC-CA, respectively). This result further proves that the adsorption of Cd(II) by biochar is more attributed to chemisorption, which may be due to the coordination reaction and complexation reaction of Cd(II) ions with the functional groups (carboxyl, hydroxyl, etc.) on the biochar surface. Among them, MBBC-PP has the highest adsorption capacity, probably because of the inner coordination between MnO_x and Cd(II).

3.3 Characterizations and Mechanisms for Cd(II) Adsorption on Modified Biochars

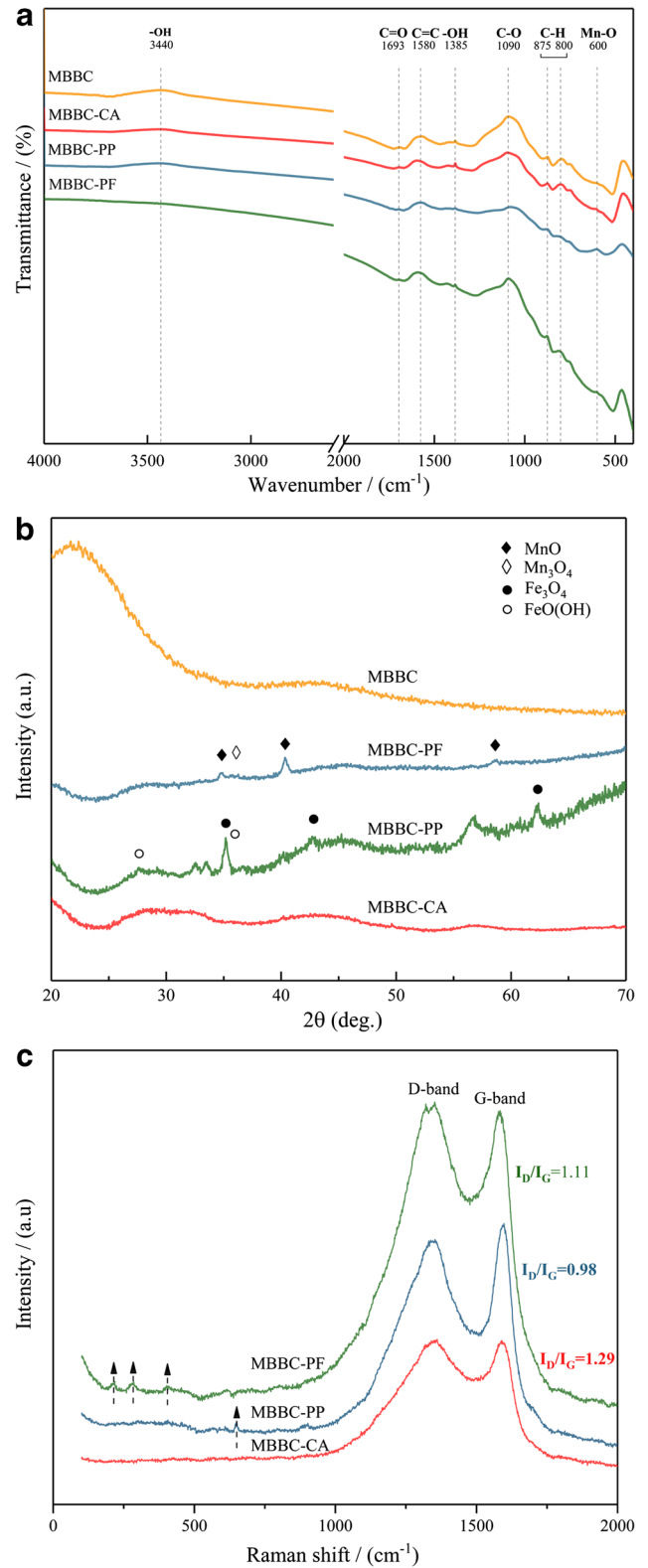
FTIR spectroscopy was used to obtain information on the variety of functional groups present on the surfaces of adsorbents. Figure 4a reveals the changes of pre- and post-modification biochars in surface functional groups. The FT-IR spectrum of MBBC demonstrates the characteristic peaks at 3340 (–OH), 1693 (aromatic C=O), 1580 (aromatic C=C), 1385 (aromatic –OH), 1090 (C–O), 875, and 800 (aromatic C–H) cm^{-1} , indicating that the surface of pristine biochar was enriched with functional groups. A distinct similarity was found between

MBBC-CA and MBBC, which presented they shared resemble types of surface functional groups and abundance. Xu et al. (2016) reported that citric acid could be applied to modify the surface of various adsorbents by introducing additional carboxyl groups onto their surfaces. However, no obvious stretching vibrations of carboxyl groups were found on the surface of MBBC-CA, probably due to the properties of biomass that difficult to bind with biochar. For MBBC-PF, the stretching vibrations of MBBC-PF decreased slightly, which implied the amount of functional groups decreased. With an increasing content of aliphatic structure in MBBC-PF, the surfaces became more hydrophilic, so that the surface of the material may wrap a layer of hydrated film to block the proximity of Cd(II). The FT-IR spectra of MBBC-PF did not find significant Fe–O vibration band, but the presence of FeO_x was confirmed by XRD and Raman later. By contrast, only a small quantity of oxygen-containing aliphatic groups was still retained on MBBC-PP, thus exhibiting obvious aromatic properties and hydrophobic surfaces, which was favorable for adsorption. Additionally, a new band at 600 cm^{-1} appeared, which was perhaps attributed to the Mn–O bond stretching (Wang et al. 2012). The C–O stretching band was not prominent in MBBC-PP, which suggests that carboxyl, ketone, and other carbonyl-containing moieties declined after KMnO_4 modified (Li et al. 2017a). Reduction of peak intensity of MBBC-PP may be due to the oxidation on the biomass surface by KMnO_4 , or complexation functional groups on biochar surface with Mn during heating.

The crystalline structures were investigated by XRD analysis. The powder X-ray diffraction patterns of MBBC, MBBC-PP, MBBC-PF, and MBBC-CA were shown in Fig. 4b. It should be noted that the XRD patterns of MBBC and MBBC-CA show no diffraction peaks, while MBBC-PP and MBBC-PF existed, indicating that MBBC was loaded with different crystal structures after modification with KMnO_4 and K_2FeO_4 . Obvious diffraction peaks at 2θ values of 27.38°, 35.20°, 35.48°, 42.84°, and 62.38° in MBBC-PF indicated the presence of Fe_3O_4 and $\text{FeO}(\text{OH})$, demonstrating that FeO_x was successfully loaded within biochar composite. In case of MBBC-PP, from the XRD patterns, it showed diffraction peaks at 34.91°, 40.34°, 58.58°, and 36.26, which can be assigned to MnO and Mn_3O_4 , respectively.

In Raman spectra (Fig. 4c), two characteristic peaks at 1350 cm^{-1} and 1600 cm^{-1} , corresponding to D and G

Fig. 4 **a** FTIR transmission spectra of MBBC, MBBC-PP, MBBC-PF, and MBBC-CA; **b** XRD patterns of MBBC, MBBC-PP, MBBC-PF, and MBBC-CA; and **c** Raman spectroscopy of MBBC-PP, MBBC-PF, and MBBC-CA



bands, respectively, were observed in the spectra of MBBC-PP, MBBC-PF, and MBBC-CA. D band represents the disorder and defects in the carbon lattice or the existence of amorphous carbon, while G band reveals in-plane tangential stretching of ordered sp² bonded carbon. The intensity ratio (I_D/I_G) indicates the degree of graphitization and the amount of functionalization in a carbon material (Narzari et al. 2017; Zhang et al. 2018). The intensity ratio (I_D/I_G) was 1.23, 1.11, 0.98, and 1.29 for MBBC (shown in Fig. S4), MBBC-PF, MBBC-PP, and MBBC-CA, respectively, suggesting that a considerable amount of functional groups were present on the surface of the biochar. The I_D/I_G ratio for MBBC-PP (0.98) was the lowest, indicating that the biochar had formed a high degree of graphitization. And the amount of functional groups in MBBC-PP was less than the other modified biochars owing to the oxidation of $KMnO_4$ on biomass stock or chemical interactions between MnO_x and functional groups, which was consistent with the findings of the FT-IR spectra (Fig. 4a). The I_D/I_G for the MBBC-PF is 1.11, higher than that of MBBC-PP (0.98), which demonstrates that MBBC-PF has large defect sites in its structure due to the stronger oxidation of K_2FeO_4 . In case of MBBC-CA, the I_D/I_G ratio was the highest, which reveals that a high number of functional groups are present on the surface of MBBC. It suggested that the modification of citric acid has a slight positive impact on the surface functional groups of biochar.

In addition, compared to MBBC-CA, new peaks were found in MBBC-PF and MBBC-PP. For MBBC-PP, the result of Raman spectra showed a peak at 650 cm^{-1} , indicating that manganese oxides were loaded on MBBC-PP. The XRD patterns and the FT-IR spectra all confirmed the existence of the MnO_x and Mn was present in the form of various oxides. According to the results of FT-IR and Raman spectrum, the oxygen-containing functional group was not a main contributor of Cd(II) adsorption by MBBC-PP. It has been reported that MnO_x has a strong affinity to heavy metal ions and forms an inner-sphere complexation with Cd(II), which is related to the contents of organics and mineral oxides containing in the biochar (El-Banna et al. 2018; Jiang et al. 2018). In addition, the cation- π bond interaction also contributed during the adsorption of Cd(II) by biochar produced at high temperatures (Li et al. 2017a). Therefore, the main adsorption mechanism of Cd(II) for MBBC-PP could be summarized as the

interaction between MnO_x and Cd(II) and cation- π bond interaction caused by the oxidation of $KMnO_4$ on biomass.

For MBBC-PF, peaks in Raman spectrum at 214.77 cm^{-1} , 284.54 cm^{-1} , and 403.56 cm^{-1} indicated the presence of FeO_x , suggesting that the iron oxide was successfully loaded on biochar, which was consistent with XRD. Similar to MBBC-PP, the adsorption sites generated by the loaded metal oxides play a key role in Cd(II) adsorption, but the effect of iron oxides was not so satisfactory compared to MBBC-PP. As revealed in the Raman spectra, $KMnO_4$ exhibited better surface oxidation ability of biomass than K_2FeO_4 . MBBC-PF would become more hydrophilic due to the increase in aliphatic structure, which hindered the approach of Cd(II), leading to the reduced adsorption of Cd(II). In turn, MBBC-PP had an increased aromatic structure and a more hydrophobic surface, which is beneficial to the interaction of Cd(II). In addition, it is reported that the biochar pores are easy to be blocked by iron oxides during iron oxide formation and consequently not provide sufficient adsorption sites. These reasons may result that the K_2FeO_4 modification is not so as $KMnO_4$.

In the case of MBBC-CA, different adsorption mechanisms of Cd(II) governed the adsorption process due to their modifier properties. A considerable amount of functional groups still existed on the surface of the biochar after modification according to the FT-IR and Raman spectra. Additionally, well-developed aromatic π -structures can act as π -electron donors and abundant oxygen-containing groups on the surface, participating in the sorption process (Ahmed et al. 2018). Therefore, the adsorption mechanism for MBBC-CA was mainly dependent on functional group complexation, electrostatic attraction, and its aromatic π -structures.

4 Conclusions

Millet bran biochars modified by potassium permanganate, potassium ferrate, and citric acid were successfully prepared for Cd(II) removal. For pristine biochar, a better adsorption capacity can be expected with higher pyrolysis temperature and solution pH. Compared with MBBC (5.2 mg/L), the adsorption capacities of biochar on Cd(II) were improved after $KMnO_4$ impregnation (36.5 mg/g), K_2FeO_4 impregnation (32.5 mg/g), and citric acid impregnation (18.5 mg/g), so MBBC-PP exhibited the highest uptake capacity. Three modified

biochars were pH-dependent. For MBBC-PP and MBBC-PF, a certain degree of decline in oxygen-containing functional groups indicated that the contribution of surface functional group complexation with Cd(II) is insignificant. Therefore, the metal oxides on the biochar that provide more adsorption sites played the most important roles for Cd adsorption. However, the hydrophilicity and hydrophobicity of biochar surface were the main reason for their different adsorption capacity. For MBBC-CA, the surface functional groups had hardly changed after modification. It enhanced adsorption capacity for Cd(II) because of surface complexation and its aromatic structures. Therefore, KMnO₄ impregnation was the most effective way to enhance Cd(II) removal from aqueous solutions.

Funding Information This work was financially supported by the Fundamental Research Funds for the Central Universities (No. 185206002, No. 201809706019) and the Science and Technology Infrastructure Program of Hubei Province of China (No. 2015BCA304).

References

- Ahmad, M., Lee, S. S., Dou, X., Mohan, D., Sung, J. K., Yang, J. E., & Ok, Y. S. J. B. T. (2012). Effects of pyrolysis temperature on soybean Stover- and peanut shell-derived biochar properties and TCE adsorption in water. *Bioresource Technology*, *118*, 536–544.
- Ahmed, M. B., Zhou, J. L., Ngo, H. H., Johir, M. A. H., Sun, L., Asadullah, M., & Belhaj, D. (2018). Sorption of hydrophobic organic contaminants on functionalized biochar: protagonist role of pi-pi electron-donor-acceptor interactions and hydrogen bonds. *Journal of Hazardous Materials*, *360*, 270–278.
- Al-Wabel, M.I., Al-Omran, A., El-Naggar, A.H., Nadeem, M., & Usman, A.R.A.J.B.T. (2013). Pyrolysis temperature induced changes in characteristics and chemical composition of biochar produced from conocarpus wastes. *131*, 374.
- Bagchi, D., Maji, T.K., Sardar, S., Lemmens, P., Bhattacharya, C., Karmakar, D. & Pal, S.K.J.P.C.C.PP (2017). Sensitized ZnO nanorod assemblies to detect heavy metal contaminated phytomedicines: spectroscopic and simulation studies. *19*, 2503.
- Barakat, M.A.J.A.J.O.C. (2011). New trends in removing heavy metals from industrial wastewater. *4*, 361–377.
- Chen, B., Chen, Z. & Lv, S.J.B.T. (2011). A novel magnetic biochar efficiently sorbs organic pollutants and phosphate. *102*, 716–723.
- Chen, Q., Zheng, J. W., Zheng, L. C., Dang, Z., & Zhang, L. J. (2018). Classical theory and electron-scale view of exceptional Cd(II) adsorption onto mesoporous cellulose biochar via experimental analysis coupled with DFT calculations. *Chemical Engineering Journal*, *350*, 1000–1009.
- Demirbas, A. J. J.O.H.M. (2008). Heavy metal adsorption onto agro-based waste materials: a review. *157*, 220–229.
- El-Banna, M. F., Mosa, A., Gao, B., Yin, X., Ahmad, Z., & Wang, H. (2018). Sorption of lead ions onto oxidized bagasse-biochar mitigates Pb-induced oxidative stress on hydroponically grown chicory: experimental observations and mechanisms. *Chemosphere*, *208*, 887–898.
- Fan, Z., Zhang, Q., Gao, B., Li, M., Liu, C., & Qiu, Y. (2018). Removal of hexavalent chromium by biochar supported nZVI composite: Batch and fixed-bed column evaluations, mechanisms, and secondary contamination prevention. *Chemosphere*, *217*, 85–94.
- Fu, F. & Wang, Q. J. J.O.E.M. (2011). Removal of heavy metal ions from wastewaters: a review. *92*, 407–418.
- Inyang, M., Gao, B., Yao, Y., Xue, Y., Zimmerman, A.R., Pullammanappallil, P. & Cao, X.J.B.T. (2012). Removal of heavy metals from aqueous solution by biochars derived from anaerobically digested biomass. *110*, 50–56.
- Jiang, B., Lin, Y., & Mbog, J. C. (2018). Biochar derived from swine manure digestate and applied on the removals of heavy metals and antibiotics. *Bioresource Technology*, *270*, 603–611.
- Jung, K.W., Choi, B.H., Jeong, T.U. & Ahn, K.H.J.B.T.T. (2016). Facile synthesis of magnetic biochar/Fe₃O₄ nanocomposites using electro-magnetization technique and its application on the removal of acid orange 7 from aqueous media. *220*, 672–676.
- Kim, K.H., Kim, J.Y., Cho, T.S., & Choi, J.W.J.B.T. (2012). Influence of pyrolysis temperature on physicochemical properties of biochar obtained from the fast pyrolysis of pitch pine (*Pinus rigida*). *118*, 158.
- Kim, W.K., Shim, T., Kim, Y.S., Hyun, S., Ryu, C., Park, Y.K. & Jung, J.J.B.T. (2013). Characterization of cadmium removal from aqueous solution by biochar produced from a giant Miscanthus at different pyrolytic temperatures. *138*, 266–270.
- Li, L., Quinlivan, P.A., & Knappe, D.R.U.J.C. (2002). Effects of activated carbon surface chemistry and pore structure on the adsorption of organic contaminants from aqueous solution. *40*, 2085–2100.
- Li, B., Yang, L., Wang, C. Q., Zhang, Q.P., Liu, Q.C., Li, Y.D. & Xiao, R.J.C. (2017a). Adsorption of Cd(II) from aqueous solutions by rape straw biochar derived from different modification processes. *175*, 332.
- Li, H., Dong, X., Silva, E.B.D., Oliveira, L.M.D., Chen, Y. & Ma, L.Q.J.C. (2017c). Mechanisms of metal sorption by biochars: biochar characteristics and modifications. *178*, 466–478.
- Narzari, R., Bordoloi, N., Sarma, B., Gogoi, L., Gogoi, N., Borkotoki, B., & Katak, R. (2017). Fabrication of biochars obtained from valorization of biowaste and evaluation of its physicochemical properties. *Bioresource Technology*, *242*, 324–328.
- Ni, B. J., Huang, Q. S., Wang, C., Ni, T. Y., Sun, J., & Wei, W. (2018). Competitive adsorption of heavy metals in aqueous solution onto biochar derived from anaerobically digested sludge. *Chemosphere*, *219*, 351–357.
- Paethanom, A., & Yoshikawa, K.J.E. (2012). Influence of pyrolysis temperature on rice husk char characteristics and its tar adsorption capability. *5*, 4941–4951.
- Peng, H., Gao, P., Chu, G., Pan, B., Peng, J. & Xing, B.J.E.P. (2017). Enhanced adsorption of Cu(II) and Cd(II) by phosphoric acid-modified biochars. *229*.

- Rajapaksha, A.U., Chen, S.S., Tsang, D.C.W., Zhang, M., Vithanage, M., Mandal, S., Gao, B., Bolan, N.S., & Yong, S.O.J.C. (2016). Engineered/designer biochar for contaminant removal/immobilization from soil and water: potential and implication of biochar modification. *148*, 276–291.
- Regmi, P., Garcia Moscoso, J.L., Kumar, S., Cao, X., Mao, J., & Schafran, G.J.J.O.E.M. (2012). Removal of copper and cadmium from aqueous solution using switchgrass biochar produced via hydrothermal carbonization process. *109*, 61–69.
- Shan, D., Deng, S., Zhao, T., Wang, B., Wang, Y., Huang, J., Gang, Y., Winglee, J. & Wiesner, M.R.J.J.O.H.M. (2015). Preparation of ultrafine magnetic biochar and activated carbon for pharmaceutical adsorption and subsequent degradation by ball milling. *305*, 156.
- Shinogi, Y., & Kanri, Y.J.B.T. (2003). Pyrolysis of plant, animal and human waste: physical and chemical characterization of the pyrolytic products. *90*, 241.
- Sizmur, T., Quilliam, R., Puga, A. P., Morenojimnez, E., Beesley, L., & Gomezeyles, J.L. (2015). *Application of Biochar for Soil Remediation*.
- Sun, L., Chen, D., Wan, S. & Yu, Z.J.B.T. (2015). Performance, kinetics, and equilibrium of methylene blue adsorption on biochar derived from eucalyptus saw dust modified with citric, tartaric, and acetic acids. *198*, 300–308.
- Vafakhah, S., Bahrololoom, M. E., Bazarganlari, R. & Saeedikhani, M. J. J.O.E.C.E. (2014). Removal of copper ions from electroplating effluent solutions with native corn cob and corn stalk and chemically modified corn stalk. *2*, 356–361.
- Wan, Z., Li, M., Zhang, Q., Fan, Z., Verpoort, F.J.E.S., & Research, P. (2018). Concurrent reduction-adsorption of chromium using m-phenylenediamine-modified magnetic chitosan: kinetics, isotherm, and mechanism. pp. 1–12.
- Wang, Y., Wang, X., Wang, X., Liu, M., Yang, L., Wu, Z., Xia, S., Zhao, J.J.C., Physicochemical, S.A., & Aspects, E. (2012). Adsorption of Pb(II) in aqueous solutions by bamboo charcoal modified with KMnO₄ via microwave irradiation. *414*, 1–8.
- Wang, H., Gao, B., Wang, S., Fang, J., Xue, Y. & Yang, K.J.B.T. (2015). Removal of Pb(II), Cu(II), and Cd(II) from aqueous solutions by biochar derived from KMnO₄ treated hickory wood. *197*, 356–362.
- Won, S. W., Kotte, P., Wei, W., Lim, A. & Yun, Y. S. J. B.T. (2014). Biosorbents for recovery of precious metals. *160*, 203–212.
- Xiang, J., Lin, Q., Cheng, S., Guo, J., Yao, X., Liu, Q., Yin, G., Liu, D.J.E.S., & Research, P. (2018). Enhanced adsorption of Cd(II) from aqueous solution by a magnesium oxide? rice husk biochar composite. pp. 1–11.
- Xin, H., Ding, Z.H., Zimmerman, A. R., Wang, S.S., & Gao, B.J.W.R. (2015). Batch and column sorption of arsenic onto iron-impregnated biochar synthesized through hydrolysis. *68*, 206–216.
- Xu, Y., Liu, Y., Liu, S., Tan, X., Zeng, G., Zeng, W., Ding, Y., Cao, W., & Zheng, B. (2016). Enhanced adsorption of methylene blue by citric acid modification of biochar derived from water hyacinth (*Eichornia crassipes*). *Environmental Science and Pollution Research International*, *23*, 23606–23618.
- Yang, E., Yao, C., Liu, Y., Zhang, C., Jia, L., Li, D., Fu, Z., Sun, D., Kirk, S.R. & Yin, D.J.F. (2018). Bamboo-derived porous biochar for efficient adsorption removal of dibenzothiophene from model fuel. *211*, 121–129.
- Yuan, J.H., Xu, R.K. & Zhang, H.J.B.T. (2011). The forms of alkalis in the biochar produced from crop residues at different temperatures. *102*, 3488–3497.
- Zhang, X., Fu, W., Yin, Y., Chen, Z., Qiu, R., Simonnot, M. O., & Wang, X. (2018). Adsorption-reduction removal of Cr(VI) by tobacco petiole pyrolytic biochar: batch experiment, kinetic and mechanism studies. *Bioresource Technology*, *268*, 149–157.
- Zhou, Y., Gao, B., Zimmerman, A. R., Chen, H., Zhang, M. & Cao, X.J.B.T. (2014). Biochar-supported zerovalent iron for removal of various contaminants from aqueous solutions. *152*, 538.

Publisher's Note Springer Nature remains neutral with regard to jurisdictional claims in published maps and institutional affiliations.